ELSEVIER

International Journal of Pharmaceutics 105 (1994) 113–123

international journal of pharmaceutics

Macromolecule transport in and effective pore size of ethanol pretreated human epidermal membrane

Takeshi Inamori, Abdel-Halim Ghanem *, William I. Higuchi, V. Srinivasan

Department of Pharmaceutics, College of Pharmacy, University of Utah, Salt Lake City, UT 84112, USA

(Received 5 May 1993; Modified version received 8 September 1993; Accepted 14 October 1993)

Abstract

This study has examined the transport behavior of macromolecules of up to about 18000 molecular weight (Mol. Wt) and the feasibility of using the theory of restricted diffusion of molecules through cylindrical pores to predict/characterize the pore sizes of synthetic membranes and ethanol pretreated human epidermal membrane (HEM). To minimize membrane and skin variabilities, experiments were conducted consecutively with each membrane using a two-chamber diffusion cell. Reference permeants or electrical resistance measurements were used to monitor possible membrane changes during a given set of runs. All HEM specimens exhibited the same pattern of significantly decreasing permeability with increasing polystyrene sulfonate (PSS) molecular weight. Previously obtained permeability data for ethanol pretreated HEM with polypeptides (leuprolide, CCK-8 and insulin) were found to be consistent with those for PSS; comparable permeability coefficients were observed for polypeptides and PSS's of comparable sizes. An analysis based on the theory of restricted diffusion for PSS transport across a synthetic Nuclepore® membrane yielded results consistent with the nominal pore size (~ 75 Å) of this membrane. A similar analysis of the PSS data obtained with ethanol pretreated HEM yielded estimates of effective pore size for this membrane in the range, 22–54 Å.

Key words: Polystyrene sulfonate; Polypeptide; Pore size; Ethanol pretreated human epidermal membrane; Synthetic membrane; Stokes-Einstein radius

1. Introduction

The transdermal transport of macromolecules has become of great interest with the advent of biotechnology methods in drug discovery, development, and production. Questions range from those of a basic nature such as the intrinsic rates and mechanisms for transport of polypeptides across the human stratum corneum to those of how macromolecule transport may be enhanced by chemical permeation enhancers, by iontophoresis or by other techniques.

There appears to be little published data on pore transport parameters for human epidermal membrane (HEM). Such data obtained for intact HEM, enhancer-treated HEM, and for HEM under dynamic conditions (e.g., iontophoresis; ultra-

* Corresponding author.

SSDI 0378-5173(93)E0315-H

sonic irradiation) should be of significant value in our understanding of transdermal polypeptide delivery. Recently, an attempt was made to investigate the iontophoretic transport property of a homologous series of low molecular weight polyethylene glycols through hairless rat skin and an effective pore radius of approx. 18 Å was estimated (Ruddy and Hadzija, 1992).

The current research in these laboratories has been aimed at gaining an understanding of (a) the transport behavior of polypeptides in HEM and (b) how chemical enhancers, iontophoresis, and their combination(s) may yield fluxes of potential therapeutic significance (Srinivasan et al., 1989, 1990; Ghanem et al., 1992; Kim et al., 1992). In the present report, a method has been developed using polystyrene sulfonates (Mol. Wt ranging from monomer to 18000) as probes to examine pore macromolecule transport characteristics of ethanol pretreated HEM. Parallel studies with a model membrane (Nuclepore®) and theoretical treatment of these data provide the foundation for the HEM studies. In this investigation, ethanol pretreatment of HEM was necessary to provide measurable transport rates; it is argued, however, that ethanol represents a chemical currently in use as a transdermal permeation enhancer and therefore this situation should be of significant practical interest.

2. Theory used for analysis of polystyrene sulfonate transport in porous membranes

The apparent diffusion coefficients of solutes in membrane pores may be much lower than in bulk solution if the dimensions of the pores are of the same order as those of the diffusing molecules (Bohrer et al., 1984; Idol and Anderson, 1986; Deen, 1987). This is known as 'hindered' or 'restricted' diffusion. Basically, the phenomenon involves (a) the pore wall restricting the freedom of the molecule, thereby affecting its spatial distribution within the pore, and (b) the frictional coefficient for the molecule is greater because of the proximity of the molecule to the pore wall.

Derivations of theoretical relationships (Pappenheimer, 1953; Renkin, 1954) for restrictive diffusion of spherical molecules through cylindrical pores demand several basic assumptions: (1) the diffusing particle is a rigid sphere and large compared to the solvent molecular dimensions; (2) the pore wall is smooth and uncharged; (3) the length/diameter ratio of the pore is large so that end effects contribute no appreciable resistance to the diffusional flux; and (4) the permeant concentration is sufficiently diluted so that no permeant-permeant interaction takes place. The pore-restriction diffusion theory proposes two reasons to account for the decrease in the apparent diffusion rate with increasing the Mol. Wt. First, the equilibrium concentration in a pore is generally lower than in the adjacent bulk solution, as a result of steric, electrostatic, or other interactions. Second, there is a hydrodynamic effect of the pore wall which enhances the drag on the macromolecule and reduces its mobility in the pore. Such restricted movement through membrane pores may be expressed by Renkin (1954):

$$D_P/D_F = (1 - r_s/r_p)^2\left[1 - 2.104(r_s/r_p) + 2.09(r_s/r_p)^3 - 0.95(r_s/r_p)^5\right] \quad (1)$$

where r_s and r_p are the radii of the diffusing permeant molecule and the pore, respectively; D_P is the effective diffusion coefficent of the permeant in the pore and D_F is that in a pore of infinite dimensions. From the D_F value, r_s (Stokes radius) can be calculated using the Stokes-Einstein equation (Deen and Smith, 1982):

$$D_F = kT/6\pi\eta r_s \quad (2)$$

where, k is Boltzmann's constant, T denotes the absolute temperature, and η is the solvent viscosity.

3. Experimental

3.1. Materials

Materials used in this study were polystyrene sulfonates (sodium salt, PSS, Polysciences, Inc., PA) of standard molecular weight with a degree of sulfonation > 90 (determined by X-ray fluorescence by the manufacturer): 206 (monomer

styrene sulfonate), nominal molecular weights 1800 (weight-average molecular weight (M_w) = 1580; number-average molecular weight (M_n) = 1394; peak molecular weight (M_p) = 1515), 5000 (M_w = 5000; M_n = 4580; M_p = 5370), 8000 (M_w = 7780; M_n = 7130; M_p = 8240) and 18000 (M_w = 17500; M_n = 16800; M_p = 18500); [^{14}C]tetraethylammonium bromide (TEAB) and [^{14}C]sucrose (New England Nuclear, MA); benzoic acid (Sigma Chemical Co., MO); ethanol (200 proof, Quantum Chemical Co., IL); polyvinylidene fluoride membrane (PVDF, 1100 Å pore radius, Millipore Co., MA); Nuclepore® membrane (75 Å nominal pore radius, Nuclepore® Co., CA); dialysis membranes (Mol. Wt cut off 6000–8000 and 12000–14000, Spectrum Medical Industries Inc., CA) and heat-separated human epidermal membrane (HEM) as described by Sims et al. (1991). Aqueous medium used in all diffusion experiments was 0.1 M phosphate-buffered saline with 0.02% sodium azide at pH 7.4.

3.2. Diffusion coefficient (D_F) determinations

The D_F for each of the permeants in dilute solution was determined using a suitably designed diffusion cell. Ten PVDF membranes were soaked in the buffer solution under vacuum for 15 min and were stacked together between the two half cells. Each half (2.7 ml volume) was stirred with a magnetic bar (8 × 2 × 2 mm placed at the bottom of the diffusion cell and at a distance of 15 mm from the diffusion membrane) using a common laboratory magnetic stirrer (150–200 rpm, VWR Dylastir). This system was used throughout an entire series of runs without disassembling. For calibration purposes, diffusion experiments were carried out at 37°C using tracer levels of [^{14}C]-sucrose in the buffer medium (and the radioactivity measured by liquid scintillation counting) and 0.1% benzoic acid (in 0.01 M hydrochloric acid and analyzed spectrophotometrically at $\lambda = 274$ nm). The benzoic acid and/or [^{14}C]sucrose runs were conducted with each cell both at the beginning and at the end of each series of PSS experiments. Experiments with PSS were conducted in the 0.1 M phosphate-buffered saline with 0.02% sodium azide at pH 7.4 and 37°C. The donor chamber PSS concentration was typically 1 mg/ml, which was believed to be low enough, even for the highest molecular weight PSS studied, to approximate the infinite dilution D_F value (Wang and Yu, 1988). The diffusion experiments were carried out successively starting with the highest PSS molecular weight, and the cell was rinsed thoroughly between runs for 20–24 h. Each experiment was conducted over a period of 1–3 h and at predetermined time intervals, aliquots were removed from the donor and receiver chambers for analysis spectrophotometrically (at $\lambda = 256$ nm for the monomer styrene sulfonate and at $\lambda = 226$ nm for polyelectrolytes).

The D_F values were calculated using the following procedure. First, P_T, the total permeability coefficient was calculated from:

$$P_T = \left(\frac{dC_R}{dt}\right)\left(\frac{V_R}{S}\right)\left(\frac{1}{C_D}\right) \tag{3}$$

Here dC_R/dt is the linear change in C_R, the PSS concentration in the receiver chamber (and corrected for sampling dilution) with time (t), C_D represents the donor PSS concentration, V_R is the receiver chamber volume, and S denotes the effective diffusional area.

P_T is related to the diffusion cell membrane permeability coefficient, P_M, by (Lin and Deen, 1992):

$$\frac{1}{P_T} = \frac{1}{P_M} + BLR \tag{4}$$

where BLR is the effective boundary layer resistance.

Further, we may write

$$P_M = \frac{D_F \epsilon}{h\tau} \tag{5}$$

where ϵ, τ, and h are the effective porosity, tortuosity, and thickness, respectively, of the membrane. The factor, $\epsilon/(h\tau)$ was assumed to be constant for all permeants with the given membrane.

Finally, we may write

$$\mathrm{BLR} = (\mathrm{BLR})_{BA}(D_{F,BA}/D_F)^n \tag{6}$$

where $(BLR)_{BA}$ is the effective boundary layer resistance for benzoic acid (BA) and $D_{F,BA}$ rep-

resents the benzoic acid diffusion coefficient. The exponent, n, depends upon the hydrodynamics in the diffusion cell chambers and will be discussed later. $(BLR)_{BA}$ was estimated by measuring the dissolution rate of a compressed benzoic acid pellet mounted on the opening of one half of the two-chamber diffusion cell (following the procedure of Yu et al., 1979). $(BLR)_{BA}$ was estimated in this manner to be $5.7 \pm 1.2 \times 10^3$ s/cm ($n = 8$) for the present diffusion cell system (noting there are two boundary layers in the diffusion cell context).

3.3. Permeability experiments

Membrane permeability experiments were conducted over a period of 1–2 h with Nuclepore® membrane, 1–12 h with dialysis membranes and 12–24 h with ethanol pre-treated HEM using the same diffusion cell and essentially the same procedure as described for the diffusion coefficient experiments. The HEM was treated with 100% ethanol for 2 h, then washed several times with the buffer. To minimize variability, a protocol was adopted where the same membrane assembled in the cell was used throughout the study after rinsing with the buffer between runs (over a period of 20–24 h).

For HEM, two sets of studies were conducted. In the first set (HEM-A), HEM samples were selected on the basis of physical appearance only (including examination for the absence of visible holes). As many as six successive experiments were carried out and HEM stability was confirmed by comparing the first and last runs with TEAB as the permeant to validate the quality of the data. HEM data which exhibited more than 50% change in TEAB permeability before and after consecutive runs were rejected.

In the second set of HEM experiments (HEM-B), the studies were conducted under more controlled conditions, first by selecting the HEM on the basis of electrical resistance and then by monitoring the electrical resistance before, during, and after each run. The resistance was determined using a four-electrode potentiostat (Srinivasan et al., 1989, 1990; Sims et al., 1991; Peck et al., 1993a): the current produced by applying 100 mV (for 2 s) was recorded, and the resistance was calculated using Ohm's law. Initially, a large number of cells ($n = 45$) were assembled and those with 25–50 kΩ cm^2 ($n = 16$) were subjected to ethanol (100%) treatment for 2 h and rinsed with buffer over a period of 24 h and resistance was recorded. The HEM resistance during the first 4–8 h after the ethanol pretreatment fluctuated then became constant. It was observed that the ethanol pretreatment generally lowered the resistance by about two orders of magnitude: this is consistent with the increase in the P_T values of TEAB after ethanol pretreatment previously found under similar experimental conditions (Srinivasan et al., 1989, 1990). The best eight cells with close resistance values were then selected for the consecutive permeability studies starting with the highest PSS molecular weight, and the resistances were monitored throughout the study.

The total permeability coefficient (P_T) was calculated using Eq. 3 as described for the diffusion coefficient. P_M was then calculated from Eq. 4 and the BLR values from Eq. 6 as illustrated in the Appendix.

4. Results and discussion

4.1. Diffusion coefficient determinations

Table 1 presents the results of the diffusion coefficient (D_F) determinations and the corresponding Stokes radii (r_s). The D_F values were calculated from the P_T values using Eq. 4–6, using the BLR value for benzoic acid of 5.7×10^3 s/cm and an n value of 0.90 in Eq. 6 (see Appendix). The average value of the factor, $h\tau/\epsilon$, was deduced to be 0.15 ± 0.03 cm (see Appendix). The Stokes radii were calculated using Eq. 2.

The D_F value for sucrose of 7.45×10^{-6} cm^2/s agrees satisfactorily with that reported by Deen et al. (1981). It was felt that this sucrose result provided independent support for the validity of the present approach.

The choice of $n = 0.90$ in Eq. 6 deserves a brief comment. Lin and Deen (1992) in their studies used $n = 2/3$ to estimate BLR of their diffusion cell using sucrose as a reference solute, and found BLR values of $1.19–1.59 \times 10^3$ s/cm.

Table 1
The experimental permeability coefficients (P_T) calculated via Eq. 3, and the calculated diffusion coefficients (D_F) using Eq. 4–6 (see Appendix) and the radii (r_s) from Eq. 2 for polystyrene sulfonates (PSS); the boundary layer resistances (BLR) were calculated using Eq. 6

Permeant	P_T (cm/s) ($\times 10^6$) ($n = 8$)	D_F (cm^2/s) ($\times 10^6$)	r_s (Å)	BLR (s/cm) ($\times 10^{-3}$)
Benzoic acid	60.3 ± 9.3	14.00 [a]	2.38	5.70
Sucrose	33.1 ± 4.1	7.45 [b]	4.47	10.64
Styrene sulfonate monomer	60.1 ± 11.8	13.80	2.38	5.77
PSS 1800	19.8 ± 2.8	4.38	7.49	16.22
PSS 5000	11.0 ± 1.6	2.39	13.72	28.00
PSS 8000	7.8 ± 1.0	1.67	19.64	38.63
PSS 18000	5.1 ± 0.9	1.08	30.37	57.19

[a] From Yu et al. (1979).
[b] In good agreement with the reported value given by Deen et al. (1981).

However, it is clear that the hydrodynamic conditions in the present situation were quite different quantitatively and, probably, qualitatively: because in our study the cell was agitated by a magnetic bar ($8 \times 2 \times 2$ mm) placed at the bottom of the diffusion cell and at a distance of 15 mm from the diffusion membrane, while in the cited reference (Lin and Deen, 1992) the cell was agitated by an axially-mounted rotating disk of comparable area to the effective diffusional area placed in close proximity to the membrane surface. In the limit of a purely stagnant layer, n should be 1.0; and it is believed based on previous dissolution rate studies (Singh et al., 1968) for a system of similar geometry and hydrodynamics that $n = 0.90$ (rather than $n = 2/3$), may better represent the present situation. It is important to point out that, if $n = 2/3$ instead of $n = 0.90$ were used in the calculations, the D_F value for the highest (18000) molecular weight PSS (the 'worst' case situation) would only be around 17% smaller; this would not affect any principal conclusions deduced in this study.

Returning to Table 1, it is worthwhile to point out that the present PSS results are consistent with the literature. The D_F values for PSS satisfactorily agree with extrapolations of D_F data obtained by Wang and Yu (1988) for higher molecular weight PSS using quasi-elastic light scattering. Also, Lin and Deen (1992) found an r_s value of 26 Å for PSS of Mol. Wt = 16000 (at 25°C) under similar ionic strength conditions; this agrees well with the present value of 30 Å for the 18000 Mol. Wt case.

It is further noteworthy that the r_s values in Table 1 are consistent with other macromolecules of biological and pharmaceutical interest: $r_s = 11$ Å for carboxy inulin (Mol. Wt = 5200; Pikal and Shah, 1990), $r_s = 12$ Å for insulin (Mol. Wt = 5600; Xu, 1990) and $r_s = 22$ Å for lysozyme (Mol. Wt = 14500; Xu, 1990).

This result is interesting in light of the intuitive thought that PSS, a linear polyelectrolyte, may be in a 'chain-expanded' state even at an ionic strength of 0.1 M and therefore would yield r_s values significantly greater than the more compact macromolecules such as insulin. This, however, does not appear to be the case.

4.2. PSS permeability experiments with Nuclepore® and dialysis membranes

Fig. 1 presents the total permeability coefficients for PSS with the Nuclepore® membrane (nominal $r_p = 75$ Å) and dialysis membranes (Mol. Wt cut off 12000–14000 and 6000–8000). It is evident that there was a much greater molecular size effect upon P_T with the dialysis membranes than with the Nuclepore membrane: this is consistent with expectations based upon the r_s values in Table 1.

The P_T values for the highest molecular weight PSS (i.e., 18000) with the dialysis membranes are seen to be of the order of 10^4 times smaller than that for the monomer. These P_T values for PSS 18000 are regarded as being probably real but are in the range of background 'noise'. A purity check by gel filtration chromatography using a Sephadex column (G-50, Pharmacia, Uppsala, Sweden) showed one peak followed by background variations equivalent to 0.01–0.02% monomer when PSS 1800 and 18000 were examined. Such data, however, serve a useful purpose as they help to establish a basis for judging the point where P_T results (for example, with HEM) may be judged to be an artifact.

4.3. Human epidermal membrane (HEM) permeability experiments

Fig. 2 and 3 present the PSS P_T data for the HEM-A and the HEM-B series, respectively. It is evident that all skin samples showed the same pattern of significantly decreasing P_T values with increasing PSS molecular weight, thus demonstrating a high degree of hindered diffusion (compare these results with the D_F data in Table 1). Large variations in P_T values were found in the HEM-A series, but the ranges of P_T variations were much narrower for the HEM-B series for which HEM samples were pre-selected on the basis of electrical resistance (i.e., 25–50 kΩ cm^2 range). In 13 out of 17 runs in the HEM-A series and in five out of eight runs in the HEM-B series,

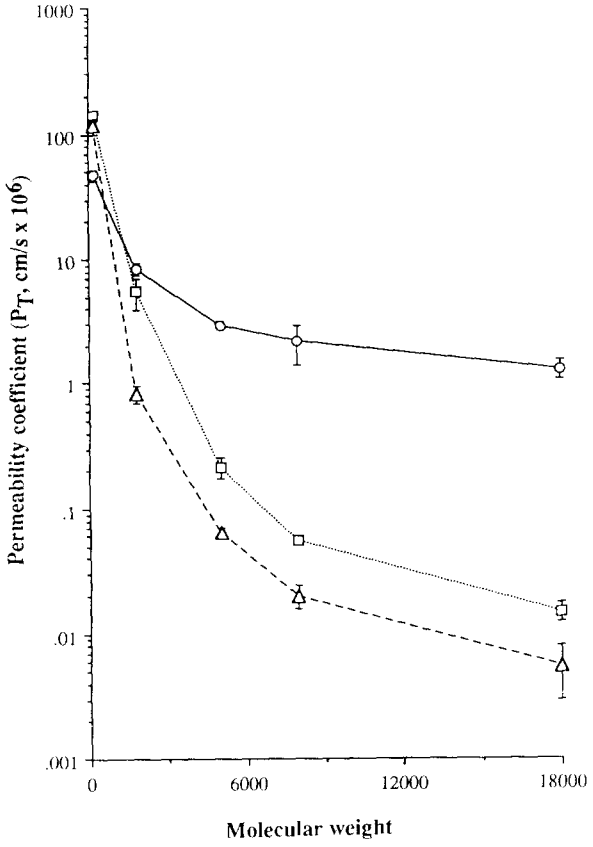

Fig. 1. Polystyrene sulfonate permeability experiments (mean and standard deviation for $n = 6$) with Nuclepore® membrane (○), and dialysis membranes of molecular weight cut off 12000–14000 (□) and of 6000–8000 (△).

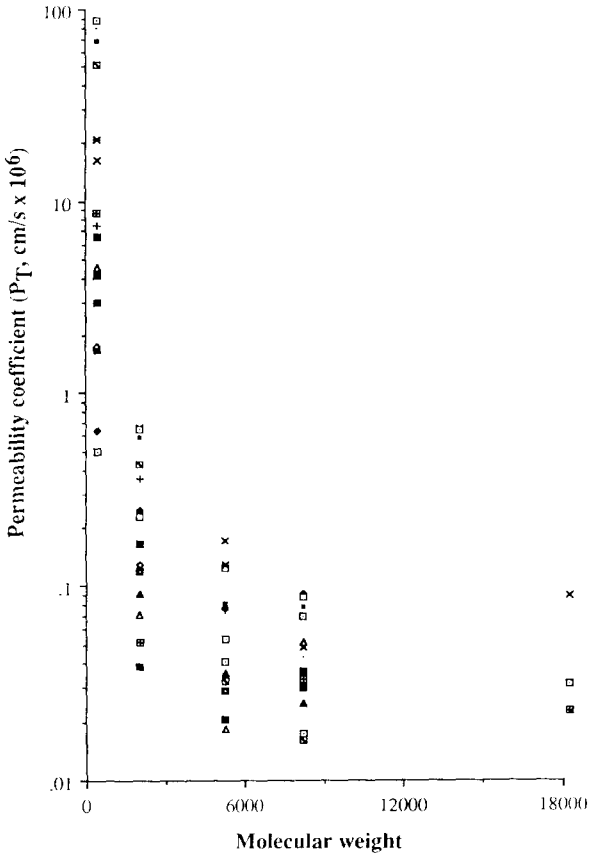

Fig. 2. Polystyrene sulfonate/ethanol pretreatment human epidermal membrane (HEM-A series) permeability experiments: All skin specimens ($n = 17$) are represented by the given symbols.

PSS 18000 Mol. Wt did not yield fluxes distinguishable from background. For all other PSS runs, fluxes were determinable and believed to be meaningful measures of the particular PSS permeability. In light of the results with the dialysis membranes (see Fig. 1) and excluding the PSS 18000 data, it is believed that neither PSS polydispersity effects nor impurities were of sufficient importance to contribute large uncertainties (i.e., artifact effects) to these results.

Table 2 presents the resistance data for the HEM-B series obtained before and after ethanol pre-treatment and during the runs. Two points may be made here: (1) there is uniformly a 100–200-fold reduction in resistance with ethanol pretreatment as noted previously (Srinivasan et al.,

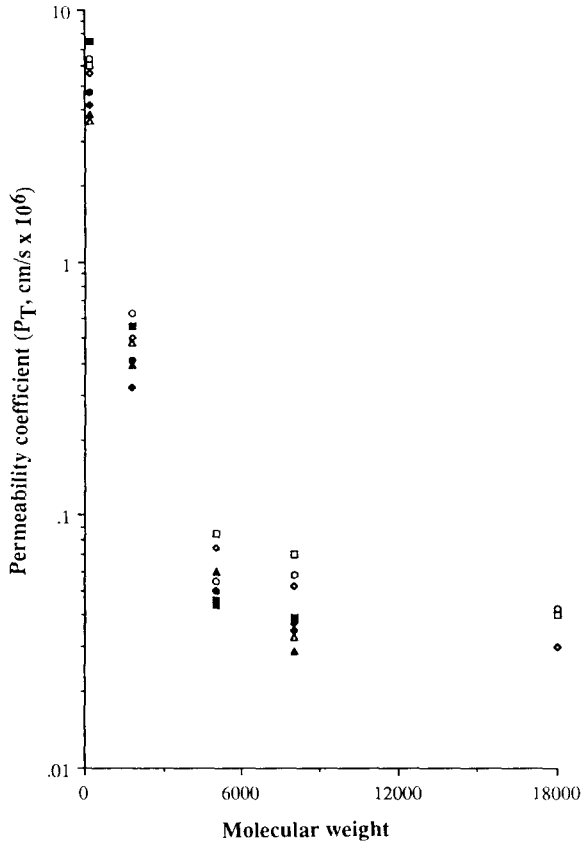

Fig. 3. Polystyrene sulfonate/ethanol pretreated human epidermal membrane (HEM-B series) permeability experiments: All skin specimens ($n = 8$) are represented by the given symbols.

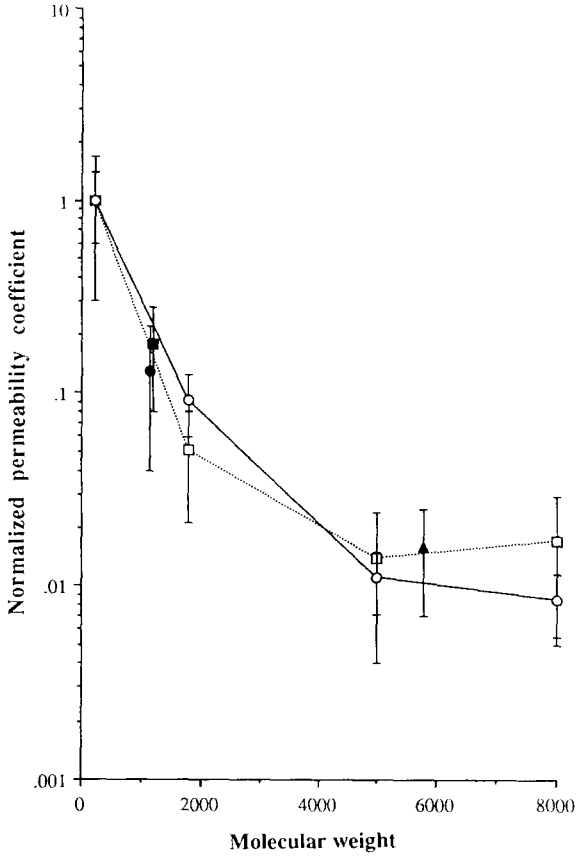

Fig. 4. Comparison of the normalized permeability coefficients for polypeptides with those for polystyrene sulfonates (PSS) obtained using ethanol pretreated human epidermal membrane (HEM). (□) PSS data from HEM-A series but including only the low TEAB permeability cases ($n = 8$); (○) PSS data from HEM-B series ($n = 8$); (■) leuprolide ($n = 3$); (●) CCK-8 ($n = 3$); and (▲) insulin ($n = 2$).

Table 2
Resistance of human epidermal membranes (HEM-B series) before (initial), after ethanol pretreatment and during PSS experiments

Skin specimens	Initial resistance (kΩ cm^2)	Resistance (kΩ cm^2) after ethanol pretreatment					
		Before 18000	After 18000	After 8000	After 5000	After 1800	After monomer
1	50.0	0.41	0.47	0.34	0.30	0.36	0.33
2	35.7	0.40	0.34	0.40	0.37	0.34	0.33
3	31.1	0.40	0.31	0.34	0.31	0.32	0.33
4	27.9	0.37	0.42	0.48	0.36	0.37	0.35
5	33.7	0.28	0.29	0.28	0.28	0.30	0.27
6	49.0	0.24	0.29	0.32	0.29	0.29	0.25
7	42.7	0.23	0.23	0.26	0.26	0.29	0.22
8	26.9	0.21	0.22	0.22	0.20	0.21	0.21

1989, 1990) and (2) in most cases the resistances remained relatively constant from the first run (Mol. Wt 18000) to the last (monomer). These results and those in Fig. 3 have made clear the benefits of using electrical resistance for selecting HEM samples and for monitoring their behavior during a series of permeability experiments.

As the primary, ultimate goal of this research is to understand the transport behavior of polypeptides and proteins in HEM, it is instructive to compare these PSS results with previously obtained data (Srinivasan et al., 1989, 1990) on the transport of leuprolide (a LHRH analogue,

Mol. Wt = 1209.4), cholecystokin-8 analogue (CCK-8, Mol. Wt = 1150.2), and insulin (Mol. Wt = 5766). In Fig. 4, permeability coefficients for PSS from the present studies are compared to the polypeptide data. To permit meaningful comparisons, the permeability coefficients were normalized by dividing the P_T value by either the monomer P_T value (HEM-B series) or by the TEAB P_T value (HEM-A series and the polypeptide results). It has been shown (unpublished data) that TEAB and the monomer have comparable P_T values with HEM under present ionic strength conditions. Also, for the HEM-A series, only the low TEAB P_T cases (the lowest eight) up to and including PSS 8000 were included. For the HEM-B, all of the results up to and including PSS 8000 were included. The plots shown in Fig. 4 demonstrate a good correlation between the previously obtained polypeptide data (Srinivasan et al., 1989, 1990) and the present PSS results. At first thought, this good correlation may seem surprising; but upon reflection, arguments may be presented in support of this good correlation. PSS 1800, leuprolide, and CCK-8 are likely rod-like molecules in solution (as opposed to being compact and spherical). Shape and 'chain expansion' effects on transport may thus be similar for the two smaller polypeptides and PSS 1800. Also, it may be shown from Table 1 that the Stokes radii for low molecular weight PSS are not too different from those of equivalent volume spheres; thus, shape and chain expansion effects are likely small to begin with for the low molecular weight macromolecules. With regard to electrostatic effects in the pores, it was recently (Hoogstraate et al., 1991) pointed out that a reversal of charge of the negatively charged membranes (Nuclepore® membranes and HEM) due to adsorption of the positively charged leuprolide (see, e.g., Idol and Anderson, 1986) was the likely cause of the reversal of the direction of the electro-osmosis driven solvent flow. Thus, it is likely that positively charged leuprolide would experience repulsive electrostatic interactions in the HEM pores, analogous to the PSS in the HEM pores.

Insulin is a more compact molecule and would be expected to be more sphere-like in transport. Why, therefore, insulin seems to correlate with PSS behavior is more difficult to rationalize. This may reside in the fact that the Stokes radius of PSS 5000 is probably still not very far (i.e., within a factor of two) of that for a compact, equivalent molecular weight sphere.

Future work should involve polypeptide flux determinations as part of a protocol, such as that used in the HEM-B series. Outcomes, then, could be data of higher precision than those in Fig. 4.

Table 3
The computed pore radii (r_p) for Nuclepore® membrane using methods A and B

Molecular weight	Method A [a]		Method B [b]	
	r_p (Å) (Eq. 1)	r_p (Å) (Munch et al. [c])	r_p (Å) (Eq. 1)	r_p (Å) (Munch et al. [c])
1800	31	83	36	67
5000	43	84	49	71
8000	63	105	75	98
18000	87	125	105	127

[a] The ratio D_P/D_F was used with Eq. 1.
[b] The ratio $(P_M/D_F)_{polymer}/(P_M/D_F)_{monomer}$ was used with Eq. 1.
[c] Corrected for the electrostatic interaction between the polyelectrolyte and the membrane by adding $1/\kappa$ to r_s and subtracting $1/\kappa$ from r_p as suggested by Munch et al. (1979).

4.4. Analysis of the Nuclepore® membrane PSS permeability data and calculation of effective pore size

Although there are fundamental limitations in applying Eq. 1 to the present situation (see Deen, 1987; Lin and Deen, 1992 for discussion of theoretical and practical difficulties associated with using Eq. 1 for permeants such as PSS), the following semi-quantitative analysis should be instructive. It importantly provides the basis for later applying Eq. 1 to the ethanol pretreated HEM data.

The following procedures were followed to estimate r_p, the effective pore radius, using the data in Table 1 with Eq. 1.

4.4.1. Method A. P_M values were obtained from the P_T values (Fig. 1) using Eq. 4 and the BLR values given in Table 1. Then, $h\tau/\epsilon = 0.135 \pm 0.025$ cm for the Nuclepore® membrane obtained

from the P_M values with the known permeants (benzoic acid and sucrose) was used to calculate D_P for the PSS. This D_P value and the D_F and r_s values from Table 1 were then used to calculate r_p using Eq. 1. A variation of method A was to account for electrostatic repulsion by adding $1/\kappa$ to r_s and subtracting $1/\kappa$ from r_p as suggested by Munch et al. (1979). Here $1/\kappa = 10$ Å is the Debye-Huckel thickness of the diffuse double layer for the present ionic strength conditions.

4.4.2. Method B. This procedure was also considered, in anticipation of the HEM data analysis for which large variations in $h\tau/\epsilon$ were expected. Here, the ratio, $(P_M/D_F)_{PSS}/(P_M/D_F)_{monomer}$, was used together with Eq. 1 to calculate r_p.

The results of both methods A and B with and without the Munch modification are presented in Table 3. The nominal pore radius for the Nuclepore® membrane is 75 Å. However, some investigators (Malone and Anderson, 1978; Deen et al., 1981; Deen and Smith, 1982; Bohrer et al., 1984) have reported significantly larger (20% larger and more, in some instances) pore sizes for Nuclepore® 75 Å. The results in Table 3 suggest that electrostatic interactions are likely quite significant and that the Munch correction, though a crude approximation, gives (together with Eq. 1) r_p values that are in the expected range. The trend of larger r_p with increasing PSS molecular weight may be rationalized on the basis of the approximate nature of Eq. 1, the crudeness of the Munch approximation, and other factors such as the appropriateness of r_s values for macromolecules obtained from unhindered diffusion for calculations in small pores (e.g., solid vs porous spheres), and not considering effects of PSS conformation distributions in small pores. Nevertheless, the results in Table 3 are believed to be encouraging enough to justify examining the application of Eq. 1 to the ethanol pretreated HEM data.

4.5. Application of Eq. 1 in estimating pore sizes of ethanol pretreated HEM

Table 4 presents the results of the application of Eq. 1 with and without the Munch correction to HEM data from the HEM-B series (Fig. 3).

Table 4
The computed ethanol-pretreated human epidermal membrane (HEM-B series) pore radii (r_p) using method B [a]

Skin specimens	r_p (Å) (Eq. 1)			r_p (Å) (Munch et al.) [b]		
	PSS 1800	PSS 5000	PSS 8000	PSS 1800	PSS 5000	PSS 8000
1	25	27	43	45	44	63
2	33	29	43	54	47	63
3	24	27	46	44	45	56
4	24	30	43	44	48	63
5	24	28	41	43	46	60
6	26	31	41	46	49	60
7	22	25	38	41	41	56
8	22	28	43	41	46	62

[a] The ratio $(P_M/D_F)_{polymer}/(P_M/D_F)_{monomer}$ was used with Eq. 1 for each skin specimen.
[b] Corrected for electrostatic interaction between the polyelectrolyte and the membrane by adding $1/\kappa$ to r_s and subtracting $1/\kappa$ from r_p as suggested by Munch et al. (1979).

Here method B was employed, i.e., the ratio $(P_M/D_F)_{PSS}/(P_M/D_F)_{Monomer}$ was used with Eq. 1 with and without the Munch correction. The r_p values presented in Table 4 are for each skin specimen. It is believed that a rigorous attempt at an error analysis is not justified at this time in light of both large uncertainties in the theory and the large variabilities in the input data.

These calculations do suggest that the effective pore sizes in ethanol pretreated HEM are in the range, 22–54 Å (giving somewhat less weight to the 8000 result of 38–63 Å). These values appear to be consistent in magnitude with (but somewhat greater) those suggested for hairless rat ($r_p = 18$ Å, Ruddy and Hadzija, 1992) and for hairless mouse ($r_p = 8$–27 Å, Pikal, 1990) both obtained from iontophoresis studies.

Recent studies in our laboratory (Peck et al., 1993b) bear importantly on the present results. The authors measured the permeation of urea, mannitol, sucrose, and raffinose across ethanol pretreated HEM under otherwise similar conditions and employed Eq. 1 to calculate r_p: r_p estimates of 15–20 Å were obtained for ethanol pretreated HEM. The r_p values in Table 1, while of the same order of magnitude as those deduced by Peck et al., are generally somewhat greater (i.e., 22–54 Å vs 15–20 Å). The following are

suggested as reasons for the differences. First, Eq. 1 is based upon the 'centerline approximation' and is expected to be accurate for only $r_s/r_p \lesssim 0.40$ (Deen, 1987); this would raise doubts about the r_p calculations using PSS molecules greater than 1800 Mol. Wt. Secondly, Eq. 1 is for solid spheres and the case for diffusing polymers and for polymers with modest segment numbers remain to be clarified (Malone and Anderson, 1978; Bohrer et al., 1984). Thirdly, a distribution of pore sizes may exist; probe permeants of larger molecular size would then yield a larger average pore size than those determined with smaller molecular permeants. Finally, the Munch approximation is a crude approximation and, for ethanol pretreated HEM pores, it may represent an overcorrection of the electrostatic effects (Deen and Smith, 1982). Future permeation studies with polyethylene glycols (Ruddy and Hadzija, 1992) of low to moderate molecular weights should help resolve some of these issues.

5. Appendix

A1. Calculation of D_F

Substitution of Eq. 5 and 6 into Eq. 4 gives:

$$\frac{1}{P_T} = \frac{1}{D_F \epsilon/(h\tau)} + (\mathrm{BLR})_{BA}(D_{F,BA}/D_F)^n \qquad (A1)$$

Here, $h\tau/\epsilon = 0.15$ cm (as shown below), $(\mathrm{BLR})_{BA} = 5700$ s/cm and $D_{F,BA} = 14.0 \times 10^{-6}$ cm^2/s (from Table 1).

Therefore,

$$\frac{1}{P_T} = \frac{0.15}{D_F} + 5700\left(\frac{14.0 \times 10^{-6}}{D_F}\right)^{0.9} = \frac{0.15}{D_F} + \frac{0.244}{D_F^{0.9}} \qquad (A2)$$

Rearranging Eq. A2 gives:

$$\frac{D_F}{0.15 P_T} - \frac{1.63}{D_F^{0.1}} = 1 \qquad (A3)$$

As P_T is experimentally determined, D_F can be easily calculated using Eq. A3, e.g., D_F for sucrose was estimated to be 7.45×10^{-6} cm^2/s which agrees satisfactorily with that reported by Deen et al. (1981).

A2. Calculation of $h\tau/\epsilon$ for PVDF membrane

Using Eq. A1 for BA we have:

$$\frac{1}{P_{T,BA}} = \frac{1}{D_{F,BA}\epsilon/(h\tau)} + (\mathrm{BLR})_{BA} \qquad (A4)$$

Here, as given in Table 1, $P_{T,BA} = 60.3 \times 10^{-6}$ cm/s, $D_{F,BA} = 14.0 \times 10^{-6}$ cm^2/s and $(\mathrm{BLR})_{BA} = 5700$ s/cm. Therefore, $h\tau/\epsilon = 0.15$ cm. This experimentally estimated value for $h\tau/\epsilon$ is very close to that calculated from the nominal h and ϵ values given by the manufacturer ($h = 0.12$ cm for 10 PVDF membranes, $\epsilon = 0.7$ and assuming $\tau = 1$).

6. Acknowledgement

This research was supported by NIH Grant GM 43181.

7. References

Bohrer, M.P., Patterson, G.D. and Carroll, P.J., Hindered diffusion of dextran and ficoll in microporous membranes. *Macromolecules*, 17 (1984) 1170–1173.

Deen, W.M., Hindered transport of large molecules in liquid-filled pores. *A.I.Ch.E.J.*, 33 (1987) 1409–1425.

Deen, W.M. and Smith, F.G., Hindered diffusion of synthetic polyelectrolytes in charged microporous membranes. *J. Membr. Sci.*, 12 (1982) 217–237.

Deen, W.M., Bohrer, M.P. and Epstein, N.B., Effect of molecular size and configuration on diffusion in microporous membranes. *A.I.Ch.E.J.*, 27 (1981) 952–959.

Ghanem, A.H., Mahmoud, H., Higuchi, W.I., Liu, P. and Good, W.R., The effects of ethanol on the transport of lipophilic and polar permeants across hairless mouse skin. Methods/validation of a novel approach. *Int. J. Pharm.*, 78 (1992) 137–156.

Hoogstraate, A.J., Srinivasan, V., Sims, S.M. and Higuchi, W.I., Iontophoretic behavior of leuprolide vs model permeants. *Proc. Int. Symp. Controlled Release Bioact. Mater.*, 18 (1991) 299–300.

Idol, W.K. and Anderson, J.L., Effects of adsorbed polyelectrolytes on convective flow and diffusion in porous membranes. *J. Membr. Sci.*, 28 (1986) 269–286.

Kim, Y.H., Ghanem, A.H., Mahmoud, H. and Higuchi, W.I., Short chain alkanols as transport enhancers for lipophilic and polar/ionic permeants in hairless mouse skin. Mechanisms of action. *Int. J. Pharm.*, 80 (1992) 17–31.

Lin, N.P. and Deen, W.M., Charge effects on the diffusion of polystyrene sulfonate through porous membranes. *J. Colloid Interface Sci.*, 153 (1992) 488–492.

Malone, D.M. and Anderson, J.L., Hindered diffusion of particles through small pores. *Chem. Eng. Sci.*, 33 (1978) 1429–1434.

Munch, W.D., Zestar, L.P. and Anderson, J.L., Rejection of polyelectrolyte from microporous membranes. *J. Membr. Sci.*, 5 (1979) 77–102.

Pappenheimer, J.R., Passage of molecules through capillary walls. *Physiol. Rev.*, 33 (1953) 387–418.

Peck, K.D., Ghanem, A.H. and Higuchi, W.I., Hindered diffusion of molecules through and effective pore size of ethanol pretreated human epidermal membrane. *Pharm. Res.*, 10 (1993b) (Suppl.) S256.

Peck, K.D., Ghanem, A.H., Higuchi, W.I. and Srinivasan, V., Improved stability of the human epidermal membrane during successive permeability experiments. *Int. J. Pharm.*, 98 (1993a) 141–147.

Pikal, M.J., Transport mechanisms in iontophoresis. I. A theoretical model for the effect of electroosmotic flow on flux enhancement in transdermal iontophoresis. *Pharm. Res.*, 7 (1990) 118–126.

Pikal, M.J. and Shah, S., Transport mechanisms in iontophoresis. III. An experimental study of the contribution of electro-osmotic flow and permeability change in transport of low and high molecular weight solutes. *Pharm. Res.*, 7 (1990) 222–229.

Renkin, E.M., Filtration, diffusion and molecular sieving through porous cellulose membranes. *J. Gen. Phys. Physiol.*, 38 (1954) 225–243.

Ruddy, S.B. and Hadzija, B.W., Iontophoretic permeability of polyethylene glycols through hairless rat skin: Application of hydrodynamic theory for hindered transport through liquid-filled pores. *Drug Des. Discovery*, 8 (1992) 207–224.

Sims, S.M., Higuchi, W.I. and Srinivasan, V., Skin alteration and convective solvent flow effects during iontophoresis: I. Neutral solute transport across human skin. *Int. J. Pharm.*, 69 (1991) 109–121.

Singh, P., Desai, S.J., Flanagan, D.R., Simonelli, A.P. and Higuchi, W.I., Mechanistic study of the influence of micelle solubilization and hydrodynamic factors on the dissolution rate of solid drugs. *J. Pharm. Sci.*, 57 (1968) 959–965.

Srinivasan, V., Higuchi, W.I., Sims, S.M., Ghanem, A.H. and Behl, C.R., Transdermal iontophoretic drug delivery. Mechanistic analysis and application to polypeptide delivery. *J. Pharm. Sci.*, 78 (1989) 370–375.

Srinivasan, V., Su, M.H., Higuchi, W.I. and Behl, C.R., Iontophoresis of polypeptides. Effect of ethanol pretreated of human skin. *J. Pharm. Sci.*, 79 (1990) 588–591.

Wang, L. and Yu, H., Chain conformation of linear polyelectrolyte in salt solution. Sodium polystyrene sulfonate in potassium chloride and sodium chloride solution. *Macromolecules*, 21 (1988) 3498–3501.

Xu, P., Enhanced transdermal diffusion of macromolecules, M.S. Thesis, University of Utah, Salt Lake City, UT (1990).

Yu, C.D., Fox, J.L., Ho, N.F.H., and Higuchi, W.I., Physical model evaluation of topical prodrug delivery. Simultaneous transport and bioconversion of vidarabine-5-valerate: II. Parameter determinations. *J. Pharm. Sci.*, 68 (1979) 1347–1357.